Journal of Research in Physics Vol.28, No. 3, 185-198 (1999)

Invited lecture

QUASI - STATIC STARK PROFILE AS A MODEL OF THE SPECTRAL LINE SHAPE OF HEAVY NEUTRAL NON - HYDROGEN EMITTERS

D. NIKOLIĆ, S. DJUROVIĆ, Z. MIJATOVIĆ, R. KOBILAROV and N. KONJEVIĆ*
Institute of Physics, trg Dositeja Obradovića 4, 21000 Novi Sad, Yugoslavia
**Institute of Physics, P.O. Box 68, 11080 Belgrade, Yugoslavia*

1. INTRODUCTION

In accordance with plasma line broadening theory, the shapes of isolated spectral lines of the heavy neutral emitters, in plasmas of medium and high densities are predominately the result of collisions with the plasma electrons. These electron impacts cause a symmetric profile of Lorentzian shape. Griem et al. (1962) developed a semi-classical theory for the shapes of non-hydrogen lines emitted from plasmas and broadened by the local electric fields of both electrons as well as ions. First applied to neutral helium, Griem (1962) subsequently extended theory to heavier elements. The effects on spectral line shape due to collisions of electrons with the radiating atoms were treated by an impact approximation, while influences of local electric fields generated by the plasma ions were assigned to asymmetries near the center of isolated spectral lines. Such asymmetries can be caused by the microfield-induced quadratic Stark shifts of the energy levels of the radiating atoms. Under usually encountered experimental conditions, where ion motion can be neglected for heavy element lines, local electric field due to plasma ions is treated by a quasi-static approximation. Griem (1974) developed criterium, considering plasma conditions, when time-dependent ion-fields should be used and when ion motion becomes significant. Performing numerical calculations, Griem (1974) showed that electron impact broadening is the dominant contributor to the broadening for neutral atoms, while ion broadening contributes mostly about 10% of the total line width. This is the case of medium density plasma conditions, which are realized in stabilized arcs. The ion contributions for the line shifts are somewhat greater, and the shifts both due to electron impact and ion broadening are 'red' shifts for the majority of lines. Upper levels of radiating atoms (and to a much smaller extent, the lower levels) are exposed to relatively small shifting (proportional to the square of the electric microfield strength) under the influence of the local fields from environmental ions. Such shifts, when smeared out by the electric microfield distribution (Baranger and Mozer, 1959; Mozer and Baranger, 1960; Hooper Jr., 1966; Hooper Jr., 1968*a*), cause the electron-broadened symmetric Lorentzian line shape to become slightly asymmetric and broader as well as shifted beyond position due to electron broadening. Appearance of asymmetry in spectral line profile provides the possibility for experimental separation of the quasi-static ion broadening contribution from the electron-impact broadening. The numerous experiments were devoted to assembling of width and shift data (Fuhr et al., 1972; Fuhr and Lesage, 1993; Konjević and Roberts, 1976; Konjević et al., 1984). However, very small and thus hardly noticeable asymmetries in the line profiles have been mostly ignored until investigations of Roder and Stampa (1964) on several helium lines. They utilized the difference in the intensity decays of the blue and the red wings of the lines, which was theoretically predicted by Griem et al. (1962). Namely, the asymptotic intensity distributions in the line wings of the quasi-static $j_{A,R}(x)$ profile are (Griem et al., 1962; Griem, 1974; Woltz, 1986):

$$j_{A,R}(x) = \frac{1}{\pi} \cdot \int_0^{\infty} \frac{W_R(\beta)\, d\beta}{1+\left(x - A^{4/3} \cdot \beta^2\right)^2} \approx \begin{cases} \frac{1}{\pi} \cdot x^{-2} \cdot \left[1+\left(\frac{3\pi}{4}\right) \cdot A \cdot x^{1/4}\right] & x >> 1 \\ \frac{1}{\pi} \cdot x^{-2} & x << -1 \end{cases} . \quad (1)$$

Here $j_{A,R}(x)$ denotes the profile of an isolated spectral line emitted by a non-hydrogen radiator in the quasi-static ion approximation; A (α in ref. Griem, 1974) denotes ion broadening parameter as a measure of the relative significance of ion to electron broadening. Parameter R is the ratio of the mean ion separation to the Debye length:

$$R = (36\pi)^{1/6} \cdot \sqrt{\frac{e^2}{kT_e}} N_e^{1/6} , \quad (2)$$

where k is the Boltzmann constant and T_e is the plasma electron temperature. The scaled frequency (wavelength) x is given by

$$x = \frac{\omega - \omega_{ul} - d_e}{w_e} = \frac{\lambda - \lambda_{ul} - d_e}{w_e} , \quad (3)$$

with angular frequency ω and wavelength λ; ω_{ul} is the unperturbed frequency (wavelength λ_{ul}) of the line, while d_e and w_e are electron impact shift and half-halfwidth respectively. The argument β in relation (1) denotes the field strength F in units of the normal field strength F_0, while $W_R(\beta)$ is the ion microfield distribution function (Baranger and Mozer, 1959; Mozer and Baranger, 1960; Hooper Jr., 1966; Hooper Jr., 1968*a*). Roder and Stampa (1974), measured for some neutral helium lines, the ratios $Q = j_{A,R}(x) / j_{A,R}(-x)$ for several wavelength distances $\pm x$ from the line center (d_e and w_e may be obtained from the tables of Griem, 1974) , and calculated a mean value for parameter A according to

$$A = (Q-1) \cdot \frac{4}{3\pi} \cdot x^{-1/4} . \quad (4)$$

Kelleher (1981) has used much improved instrumentation to investigate most of these and several others He I lines. With the same approach good agreement with earlier experimental results and theory was obtained. Brandt et al. (1981) also performed a similar investigation of differences in the two line wings for a neutral krypton lines, and Nubbemeyer (1980) for vacuum ultraviolet lines of neutral nitrogen. Utilizing the general theoretical line profiles calculated and tabulated by Griem (1974), Goly and Grabowski (1976) perfomed best fit procedures on the shape of several neutral carbon lines. For known plasma conditions, parameter R (Eq. 2) is also known, so using tabulated electron shifts d_e and half-halfwidths w_e (Griem, 1974) it was possible to adjust value of ion broadening parameter A by iterative interpolation of tabulated quasi-static $j_{A,R}(x)$ profiles (Griem, 1974). Goly and Grabowski (1976) thus derived, for the first time by least-square procedure, values only for ion broadening parameter A.

In Refs. (Jones and Wiese, 1984; Jones et al., 1986; Jones and Wiese, 1987; Badie and Bacri, 1991), Lorentzian profiles were fitted to the experimental and theoretical $j_{A,R}(x)$

profiles. A functional relationship between the maximum of the Lorentzian - $j_{A,R}(x)$ deviation curve and parameter A was established. This function then was used for determination of values for A from the maximum deviations between the experimental points and the fitted Lotentzian. Such deviation method uses experimental points near the maximum deviation between the experimental profile and the fitted Lorentzian, and further more requires interpolation to determine the peak of the deviation curve; this interpolation procedure can be an additional source of error. Using an alternate approach, Hahn and Woltz (1990) developed a computer code, which fits the experimental profile with an asymmetric theoretical $j_{A,R}(x)$ profile by varying the width, shift, ion broadening parameter, and the cubic background of the theoretical curve. Namely, theoretical profiles $j_{A,R}(x)$ of known A were fitted to the experimental profiles of some neutral argon and carbon lines. Theoretical profiles $j_{A,R}(x)$ were generated for three initial guesses for A (A_1, A_2 and A_3) and for a known R, determined from the plasma density and temperature. Then the parameters d_e and w_e (Eq.3) are varied to minimize the sum of squared deviations χ_i^2 (χ_1^2, χ_2^2 and χ_3^2) between the experimental and theoretical profiles for each A_i. The fitting was done within one half width at half maximum (HWHM) of the line center where the experimental data are most reliable due to large signal-to-noise ratio, and where other sources of wing asymmetries are minimal. A cubic polynomial background is fitted to the experimental points beyond one HWHM from line center. It was found that the value of A is relatively insensitive to this background as well as to the value of parameter R. The next guess for A was taken as the minimum point of a parabola fitted through the three points (A_i, χ_i^2). The worst A_i (whose χ_i^2 is the largest) is discarded and procedure was repeated until the function $\chi^2(A)$ was minimized within a given tolerance. Hahn and Woltz (1990) concluded that the quasi-static ion approximation and quadratic level shifts due to the ion microfield give a good theoretical description of the asymmetries of the spectral line profiles studied in their work, and that a proposed least-square fitting technique can be of use in determining the experimental ion broadening parameter A. Neglecting a distinctions among above mentioned techniques of various authors, one common characteristic could be emphasized: experimental methods and instrumentation were used to provide such the plasma conditions necessary for validity of quasi-static approximation for ions and domination of the Stark effect in broadening of spectral lines. The other broadening mechanisms (natural, resonance, Van der Waals, Doppler and apparatus) were either neglected or later on taken into account by the simple corrections. When the Gaussian portion (corresponding to Doppler and apparatus broadening) of the experimental profile is of the same order or greater than the Lorentzian part (arising from Stark broadening with negligible asymmetry due to ions), Voigt profiles of general type (Goly and Weniger, 1986; Bakshi and Kearney, 1989; Davies and Vaughan, 1963) can be used as model functions. When the influence of the ion broadening on the line shape can not be neglected, the important Gaussian portion have to be taken into account by folding the profile $j_{A,R}(x)$ after Griem (1974) with Gaussian profile (Goly and Weniger, 1986; Mijatović et al.,1993; Knauer and Kock, 1996; Nikolić, 1998; Schinkoth et al., 1998):

$$K(x) = \int_{-\infty}^{+\infty} G(x-s) \cdot j_{A,R}(s)\, \mathrm{d}s\,. \qquad (5)$$

It is assumed that all others broadening mechanisms are negligible; on the contrary, their resulting profiles should be also taken account by folding them with the convolution $K(x)$ (Knauer and Kock, 1996).

This paper deals with the convenience of using the model (5) with the purpose to evaluate the Stark parameters directly from the experimental profiles of isolated or overlapped spectral lines of neutral atoms. In that manner, a method used by Nikolić (1998) will be presented through the short discussion of the nonlinear fitting of synthetic and of some experimental profiles.

2. NON-LINEAR REGRESSION AS A MODELING TOOL

Common modeling application in scientific research is that of predicting an outcome on the basis of experience. This statistical method, known as regression analysis, requires that functional relationship between the dependent Y and independent X variables be specified. In the past, regression analysis has been largely limited to linear models. Such models can be solved by hand with a single matrix inversion, although they are more easily solved using a computer. Certain other models can be made linear by parameter transformation in order to utilize linear regression techniques. Such transformations can introduce unwanted and sometimes unsuspected limitations or assumptions into the model and must be used with care. The majority of models encountered in spectral line shapes research, however, are nonlinear (related to parameters of the model) and cannot be transformed into linear form. Certain requirement exists for a general-purpose non-linear regression technique, which is both sufficiently general and robust to be applicable to a wide variety of research interests.

Most of today's software for non-linear regression is based on an algorithm by Marquardt (1963), which uses a Taylor's series expansion to give successive improvements to an initial set of parameter estimates. The method is actually a compromise between the inverse Hessian matrix method (Press et al., 1995) and the method of steepest descent (gradient method). It combines the best features of both methods while avoiding theirs most serious limitations (Draper and Smith, 1966). It shares with the gradient methods their ability to converge from an initial guess which may be outside the region of convergence of other methods (Press et al., 1995) and with the inverse Hessian matrix methods their ability to rapidly converge once in the vicinity of the minimum. An attenuation parameter (ξ) is used to switch smoothly between the two methods when is needed. Making ξ large favors the gradient method, and expands the region of convergence. Making ξ small selects the inverse Hessian matrix method and favors rapid convergence. Although no single method can be considered as the best one for all non-linear problems, Marquardt's method is a sensible first choice, providing the reasonable initial parameter estimates.

The goal of nonlinear regression is to fit a model to experimental data. More precisely, the goal is to minimize the sum of the squares of the vertical distances of the points (e.g. χ^2 - function) from the model curve (MC). A model is a formal presentation of a scientific idea. To be useful for nonlinear regression, the model must be expressed as an equation that defines Y, the outcome which one measures, as a function of X and one or more parameters $\vec{p}$ that one wants to fit. Choosing a model is a scientific decision and has to be based on understanding of scientific problem and should not be based solely on the shape of the graph. The key assumption is that the data really do follow a specified MC, and

that all scatters are attributable to random variation. For least-square regression to be valid, it has to be assumed that this variation (approximately) follows a Gaussian distribution, and that the standard deviation of the scattering is the same for all parts of the MC. In other words, the degree of scattering is completely unrelated to X. Except for a few special cases, it is not possible to directly solve the χ^2 - function minimum set of equations to find the values $\vec{p}_*$ of the model parameters which minimize the χ^2 - function. Instead, nonlinear regression requires an iterative approach. Here are the steps that every nonlinear regression procedure follows:

1. Starting with an initially estimated value for each parameter $\vec{p} \equiv (p_1, p_2, \ldots p_M)$ in the model curve: $Y = Y(X; p_1, p_2, \ldots p_M)$.
2. Generating the MC determined by the initial values; after that, calculation of the value of χ^2 - function defined as, $\chi^2(\vec{p}) = \sum_{i=1}^{N} \frac{(Y_i - Y(X_i; \vec{p}))^2}{\sigma_i^2}$, where (X_i, Y_i) is the set of N experimental points and σ_i is set of their measurement errors (standard deviations).
3. Adjusting the parameters $\vec{p}$ to make the MC come closer to the data points. There are several algorithms for adjusting parameters. Levenberg and Marquardt (Press et al., 1995) derived the most commonly used method discussed in the next section.
4. Adjusting the parameters again so that MC comes even closer to the points.
5. Proceeding with step 4 until the adjustment makes virtually no difference in the value of χ^2 - function.
6. Reporting the best - fit results. The obtained precise values will depend partially on the initial values chosen in step 1, and the stopping criteria of step 5. This means that repeated analyses of the same data will not always give exactly the same results.

If obtained data are 'clean' that clearly define a curve, then it is usually doesn't matter if the initial values are fairly far from the 'correct' values. One will get the same answer no matter what initial values uses, unless the initial values are far from 'correct'. Initial values matter more when experimental data have a lot of scatter, don't span a large enough range of X values to define a full curve, or don't really fit the model. In these cases, one may get different answers depending on which initial values were used. This problem (called *finding a local minimum*) is intrinsic to nonlinear regression, no matter what procedure is used. Fitting procedure will rarely encounter a local minimum if data have little scatter or were collected over an appropriate range of X values, and an appropriate model equation is chosen . To test for the presence of a false minimum it is necessary to:

- Note the values of the parameters $\vec{p}$ and the χ^2 - function from the first fit
- Make a large change to the initial values of one or more parameters $\vec{p}$ and run the fit again
- Repeat preliminar step several times
- Ideally, procedure will report nearly the same values of χ^2 - function and same parameters $\vec{p}$ regardless of the initial values. If the values are different, the one with the lowest value of χ^2 - function should be accepted.

3. LEVENBERG - MARQUARDT METHOD

Sufficiently near to the minimum, it is reasonable to expect that the χ^2 - function can be approximated by a quadratic form due to Taylor's series expansion (Press et al., 1995):

$$\chi^2(\vec{p}) \approx \chi^2(\vec{p}_*) + \left.\frac{\partial \chi^2(\vec{p})}{\partial \vec{p}}\right|_{\vec{p}_*} \cdot (\vec{p} - \vec{p}_*) + (\vec{p} - \vec{p}_*) \cdot \left.\frac{\partial^2 \chi^2(\vec{p})}{\partial \vec{p}^2}\right|_{\vec{p}_*} \cdot (\vec{p} - \vec{p}_*), \tag{6}$$

where $\mathbf{g} \equiv \dfrac{\partial \chi^2(\vec{p})}{\partial \vec{p}}$ is an M-vector and $\mathbf{H} \equiv \dfrac{\partial^2 \chi^2(\vec{p})}{\partial \vec{p}^2}$ is an $M \times M$ (Hessian) matrix. If the approximation (6) is a good one, only one step divides the current trial parameters $\vec{p}$ from minimizing ones $\vec{p}_*$:

$$\vec{p}_* = \vec{p} + \mathbf{H}^{-1} \cdot \mathbf{g} \ . \tag{7}$$

Approximation (6) may be unfavorable for the shapes of the χ^2 - function at $\vec{p}$, so step down the gradient is necessary like in the steepest descent method:

$$\vec{p}_{next} = \vec{p} + const. \cdot \mathbf{g} \ , \tag{8}$$

where the *const.* has to small enough not to loose the direction down the χ^2 - function surface. Making the use of Eqs. (7, 8) one has to compute $\mathbf{g}$ (the gradient of the χ^2 - function at any set of model parameters $\vec{p}$), and also the matrix $\mathbf{H}$ which is the second derivative matrix of the χ^2 - function at any $\vec{p}$. To do so, one has to specify the model curve $Y = Y(X; \vec{p})$ and the $\chi^2(\vec{p})$ merit function. The gradient of $\chi^2(\vec{p})$ with respect to the parameters $\vec{p}$ has the components:

$$[\mathbf{g}]_q \equiv \frac{\partial \chi^2}{\partial p_q} = -2 \sum_{i=1}^{N} \frac{(Y_i - Y(X_i; \vec{p}))}{\sigma_i^2} \cdot \frac{\partial Y(X_i; \vec{p})}{\partial p_q} \qquad q = 1, 2, \ldots M, \tag{9}$$

while after taking additional derivatives, Hessian matrix has the components:

$$[\mathbf{H}]_{sq} \equiv \frac{\partial^2 \chi^2}{\partial p_s \partial p_q} = 2 \sum_{i=1}^{N} \frac{1}{\sigma_i^2} \cdot \left[\frac{\partial Y(X_i; \vec{p})}{\partial p_s} \cdot \frac{\partial Y(X_i; \vec{p})}{\partial p_q} - (Y_i - Y(X_i; \vec{p})) \cdot \frac{\partial^2 Y(X_i; \vec{p})}{\partial p_s \partial p_q} \right] \tag{10}$$

$$s, q = 1, 2, \ldots M$$

It is common in practice to introduce new components of gradient and Hessian:

$$\beta_q \equiv -\frac{1}{2} \cdot [\mathbf{g}]_q \quad \text{and} \quad \alpha_{sq} \equiv \frac{1}{2} \cdot [\mathbf{H}]_{sq}, \tag{11}$$

so that Eq.(7) can be rewritten in terms of the increments $\delta\vec{p} = \vec{p}_* - \vec{p}$ as the set of linear equations:

$$\sum_{q=1}^{M} \alpha_{sq} \cdot \delta p_q = \beta_s \qquad s = 1, 2, \ldots M . \tag{12}$$

After solving the set (12) for the increments $\delta\vec{p}$, adding them to the current approximation for parameters $\vec{p}$ it is possible to get the next approximation ($\vec{p}_{next} = \vec{p} + \delta\vec{p}$). Equation (8), the steepest descent formula, translates to:

$$\delta p_q = const. \cdot \beta_q \qquad q = 1, 2, \ldots M . \tag{13}$$

Curvature matrix $[\alpha]$ has the components dependant both on the first and on the second derivatives of the model curve with respect to the model parameters (Eq. (10)). The second derivative term can be dismissed when it is zero (model curve depends linearly on parameters $\vec{p}$) or small enough comparing to the first derivative term. An additional possibility arises in practice, when the term $\left(Y_i - Y_i(X_i;\vec{p})\right)$, multiplying the second derivative in Eq. (10), is sufficiently small for a successful model because this term should be the random measurement error of each point. This error can have both signs, and in general should be uncorrelated with the model, so that the second derivative terms tend to cancel out each other when summed over *i*. Following the definition of curvature matrix components, next relation will be used instead Eq. (11):

$$[\alpha]_{sq} = \sum_{i=1}^{N} \frac{1}{\sigma_i^2} \cdot \left[\frac{\partial Y(X_i;\vec{p})}{\partial p_s} \cdot \frac{\partial Y(X_i;\vec{p})}{\partial p_q} \right] \qquad s = 1, 2, \ldots M . \tag{14}$$

From the fact that the χ^2 - function is nondimensional, the constants of proportionality between δp_q's and β_q's in Eq. (13) therefore must have dimensions of p_q^2 since β_q have dimension of p_q^{-1}. According to definition (14) for the components of $[\alpha]$, only the reciprocals of the diagonal elements $1/\alpha_{qq}$ have the dimensions of p_q^2. Levenberg-Marquardt method is based on the two facts. First is that the *const.* in Eq. (13) should be replaced with $\frac{1}{\xi \cdot \alpha_{qq}}$, where the attenuation nondimensional parameter ξ serves to cut down the step (setting $\xi >> 1$), and the second one is that eqs. (12,13) can be built into only one set of linear equation for increments $\delta\vec{p}$:

$$\sum_{q=1}^{M} \alpha'_{sq} \cdot \delta p_q = \beta_s \qquad s = 1, 2, \ldots M , \tag{15}$$

where the new curvature matrix $[\alpha']$ is defined by the following prescription:

$$\alpha'_{sq} \equiv (1 + \xi \cdot \delta_{sq}) \cdot \alpha_{sq} \qquad s, q = 1, 2, \ldots M , \tag{16}$$

where δ_{sq} is the Kronecker's symbol. When ξ is very large, the matrix $[\alpha']$ is forced to be diagonally dominant and (16) tends to (13); on the other hand, as ξ approaches zero, Eq. (16) goes over to (12).

With the given initial guess for the set of model parameters $\vec{p}$, Marquardt (1963) recommended an effective algorithm:

- Compute $\chi^2(\vec{p})$.
- Set a modest value for ξ, commonly $\xi = 0.001$.
- (❖) Solve the set of the linear equations (15) for the increments $\delta\vec{p}$ and evaluate $\chi^2(\vec{p}+\delta\vec{p})$
- If $\chi^2(\vec{p}+\delta\vec{p}) \geq \chi^2(\vec{p})$, increase ξ by a factor of 10 and go to (❖)
- If $\chi^2(\vec{p}+\delta\vec{p}) \leq \chi^2(\vec{p})$, decrease ξ by a factor of 10, set the new trial solution $\vec{p} \leftarrow \vec{p}+\delta\vec{p}$, and go to (❖)
- Condition of stopping is determined with first or second occasion that χ^2 decreases by a negligible amount (say fractional amount like 10^{-3})
- When acceptable minimum has been found, set $\xi = 0$ in order to compute estimated covariance matrix $[C] \equiv [\alpha]^{-1}$ of standard errors in the fitted parameters $\vec{p}$ (Press et al., 1995).

4. EVALUATION OF STARK PARAMETERS

According to Section 1 of this work and under conditions mentioned therein, it is reasonably to assume that isolated spectral lines of neutral emitters could be modeled by Eq. (5). This model has to be accommodated to real experimental situations. Experimental profiles are mostly represented as some relationship between signals from detector and wavelength of observed radiation. So, transition from the scaled wavelengths x to real wavelengths λ is needed. Amplitudes of signals from detector are usually normalized to maximal detected value, but almost never to the area under the experimental profile. That's why a normalized constant C_n has to be introduced. The Gaussian part of the convolution (5) decays fast on the wings, and practically tends to zero at distances of the several halfwidths from the center of the Gaussian profile. This fact justify the reduction of integration limits in (5) from $\lambda \in (0,\infty)$ to $\lambda \in (\lambda_0^* - \Delta\lambda, \lambda_0^* + \Delta\lambda)$, where λ_0^* denotes the center of the line and $\Delta\lambda$ has to be chosen in such manner to optimize accuracy of numerical integration against the computing time. The electric microfield distribution function $W_R(\beta)$ is tabulated for neutral point and charged point cases in Refs. (Hooper Jr., 1966; Hooper Jr., 1968*a*) and for the values $\beta \in (0,10)$. For $\beta > 10$ distribution function $W_R(\beta)$ is practically zero, so integration limits $\beta \in (0,\infty)$ in Eq. (1) can be replaced with limits $\beta \in [0,10]$ unless the more accurate computations have to be performed (Hoper Jr., 1968*b*). With the two-dimensional interpolation of mentioned tables for $W_R(\beta)$, it is possible to compute values of $j_{A,R}(\lambda)$ profile for given values of the parameters A and R. Since the spectral line always has underlying continuum, it is necessary to add in Eq. (5) unknown function $cont(\lambda)$, which represents continuum dependence on the wavelength. According to many laboratory experimental results, the isolated spectral lines of the neutral emitters are relatively narrow (the total halfwidths for the medium plasma conditions are

below 0.5 nm) and in the case of the Ar I lines (Nikolić, 1998) the observations were made inside of approximately eight halfwidths around the line center. In such spectral intervals it is justified to consider the continuum as independent or weakly linearly dependent function of the wavelength. Extensive simulations (Nikolić, 1998; Nikolić et al., 1998) have shown that, the preliminary subtraction of the fitted underlying continuum from the experimental profiles, do influence the adjusted values for the fitted stark parameters $\vec{p} \equiv (w_e, d_e, A)$ but always under 2%. On the other hand, such preliminary subtraction of the continuum reduces the number of the model parameters, and therefore the time needed for the overall fitting. Taking into account all the facts mentioned above, the convolution model (5) adapted for the real situations has the form:

$$\overline{K}(\lambda) \approx \frac{2\sqrt{ln2}}{\pi^{3/2} w_G} \cdot \frac{C_n}{w_e} \cdot \Psi_{1,0,0}(\lambda), \tag{17}$$

where overbar denotes continuum reduction. Here w_G means the halfwidth of the Gaussian portion of the convolution (17):

$$w_G = \sqrt{w_D^2 + w_I^2}, \tag{18}$$

with Doppler w_D and apparatus w_I broadening effects included. Concise notation has been introduced for the convolution integral (17):

$$\Psi_{a,b,c}(\lambda) \equiv \int_{\lambda_0 - \Delta\lambda}^{\lambda_0 + \Delta\lambda} d\lambda' (\lambda')^b \cdot e^{-\frac{4ln2}{w_G^2}(\lambda' - \lambda)^2} \int_0^{10} d\beta (\beta)^c \cdot \frac{W_R(\beta)}{\left[1 + \left(\frac{\lambda' - \lambda_0 - d_e}{w_e} - A^{4/3} \cdot \beta^2\right)^2\right]^a}, \tag{19}$$

where λ_0 is the wavelength corresponding to the center of the observed line emitted from the referent low pressure source (as Geissler tube, for example) . The gradient components of the model function (17) are:

$$\frac{\partial \overline{K}}{\partial w_e} = \frac{4\sqrt{ln2}}{\pi^{3/2} w_G} \cdot \frac{C_n}{w_e^4} \cdot \left[\Psi_{2,2,0} - 2 \cdot (\lambda_0 + d_e) \cdot \Psi_{2,1,0} - \gamma \cdot w_e \cdot \Psi_{2,1,2} + (\lambda_0 + d_e)^2 \cdot \Psi_{2,0,0} + \right.$$
$$\left. + \gamma \cdot w_e \cdot (\lambda_0 + d_e) \cdot \Psi_{2,0,2} - \frac{1}{2} \cdot w_e^2 \cdot \Psi_{1,0,0}\right], \tag{20}$$

$$\frac{\partial \overline{K}}{\partial d_e} = \frac{4\sqrt{ln2}}{\pi^{3/2} w_G} \cdot \frac{C_n}{w_e^3} \cdot \left[\Psi_{2,1,0} - (\lambda_0 + d_e) \cdot \Psi_{2,0,0} - \gamma \cdot w_e \cdot \Psi_{2,0,2}\right], \tag{21}$$

$$\frac{\partial \overline{K}}{\partial \gamma} = \frac{4\sqrt{ln2}}{\pi^{3/2} w_G} \cdot \frac{C_n}{w_e^2} \cdot \left[\Psi_{2,1,2} - (\lambda_0 + d_e) \cdot \Psi_{2,0,2} - \gamma \cdot w_e \cdot \Psi_{2,0,4}\right], \tag{22}$$

$$\frac{\partial \bar{K}}{\partial C_n} = \frac{2\sqrt{ln2}}{\pi^{3/2} w_G} \cdot \frac{1}{w_e} \cdot \Psi_{1,0,0} \quad , \text{ and} \tag{23}$$

$$\frac{\partial \bar{K}}{\partial w_G} = \frac{16(ln2)^{3/2}}{\pi^{3/2} w_G^4} \cdot \frac{C_n}{w_e} \cdot \left[\Psi_{1,2,0} - 2 \cdot \lambda \cdot \Psi_{1,1,0} - \lambda^2 \cdot \Psi_{1,0,0} - \frac{w_G^2}{8 ln2} \cdot \Psi_{1,0,0} \right], \tag{24}$$

where $\gamma = A^{4/3}$. The last gradient component (24) could be eliminated from fitting procedure due to the fact that the Gaussian halfwidth can be experimentally determined (Nikolić, 1998). To summarize, implementing Levenberg-Marquardt algorithm for χ^2-function minimization, it is possible to adjust fitting parameters $(w_e, d_e, \gamma, C_n, w_G)$ in such manner that convolution (17) properly describes experimental profiles of the neutral non-hydrogen emitters. Furthermore, in the case of two overlapping spectral lines similar procedure gives satisfactory results, but the fitting time is much longer, since one has the eight parameters to adjust $(w_{e1}, d_{e1}, \gamma_1, C_{n1}, w_{e2}, d_{e2}, \gamma_2, C_{n2})$. The model function in that case has the form:

$$\bar{K}(\lambda) \approx \frac{2\sqrt{ln2}}{\pi^{3/2} w_{G1}} \cdot \frac{C_{n1}}{w_{e1}} \cdot \Psi^{(1)}_{1,0,0}(\lambda) + \frac{2\sqrt{ln2}}{\pi^{3/2} w_{G2}} \cdot \frac{C_{n2}}{w_{e1}} \cdot \Psi^{(2)}_{1,0,0}(\lambda) \tag{25}$$

and the gradient components have the same form as eqs. (20-24) with the parameters corresponding to the overlapped lines. In the next section will be briefly presented several steps of the isolated synthetic spectral line profile fitting by the program code written in *Mathematica 3.0* (Wolfram, 1996) and given in Appendix 1 of ref. Nikolić (1998).

5. SIMULATIONS

For the testing purposes of given fitting procedure, discussed in the previous section, first step is to generate synthetic convolution profile defined by Eq. (17). The exact values of parameters, which are fixed during the fitting, were: $\Delta\lambda = 0.5$ nm, $w_G = 0.021$ nm and $R = 0.45$, while artificial values for adjustable parameters were $w_e = 0.025$ nm, $d_e = 0.020$ nm, $\gamma = 0.15$ and $C_n = 0.5$ arb.u.$\cdot$nm. With these values an synthetic convolution (17) was generated in $N = 100$ equally spaced points with the step of 0.005 nm. Such synthetic profile was then disturbed by a normally (Gaussian) distributed random noise centered at each point with the standard deviation of 0.01 arb.u.. This noise is almost three times larger than the experimental one (Nikolić, 1998). After that, fitting procedure was performed, accordingly to the described method, with an initial set of adjustable parameters: $w_e = 0.015$ nm, $d_e = 0.015$ nm, $\gamma = 0$ and $C_n = 0.3$ arb.u.$\cdot$nm. Fig. 1 shows the result of such initial guess. After eight iterations, with the stopping criteria that the relative change in the χ^2 value should not exceed 0.5%, optimal values were obtain; namely: $w_e = 0.0265$ nm, $d_e = 0.0217$ nm, $\gamma = 0.117$ and $C_n = 0.5025$ arb.u.$\cdot$nm. Fig. 2 shows the final result of fitting. Relative discrepancies between the artificial and fitted values are: 6% for w_e, 8.5% for d_e, 16.5% for A and 0.5% for C_n.

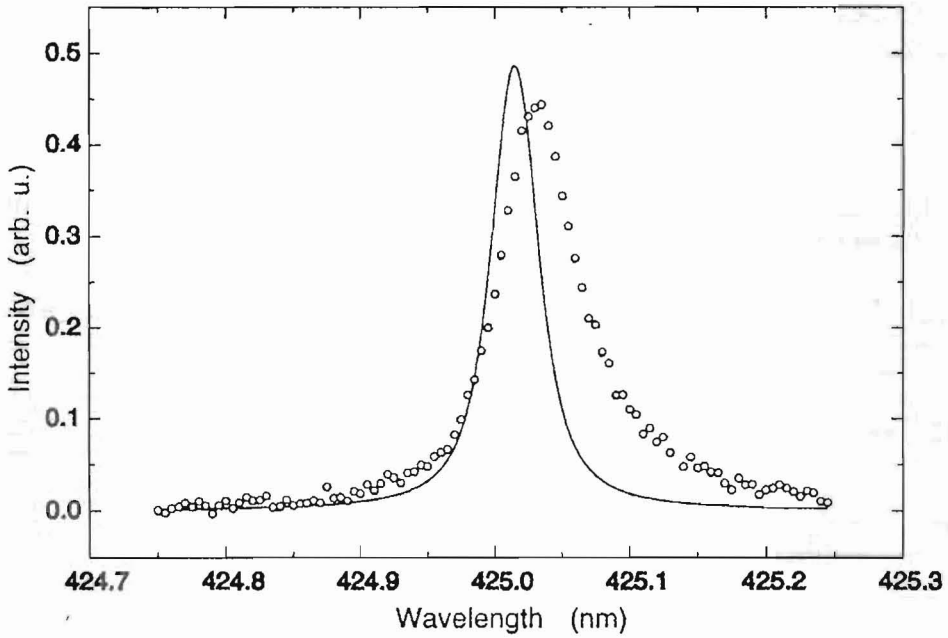

Fig. 1. Comparison of the randomly disturbed synthetic convolution (∘ ∘ ∘) with the model convolution (——) generated with an initial set of adjustable parameters: $w_e = 0.015$ nm, $d_e = 0.015$ nm, $\gamma = 0$ and $C_n = 0.3$ arb.u. · nm, before fitting.

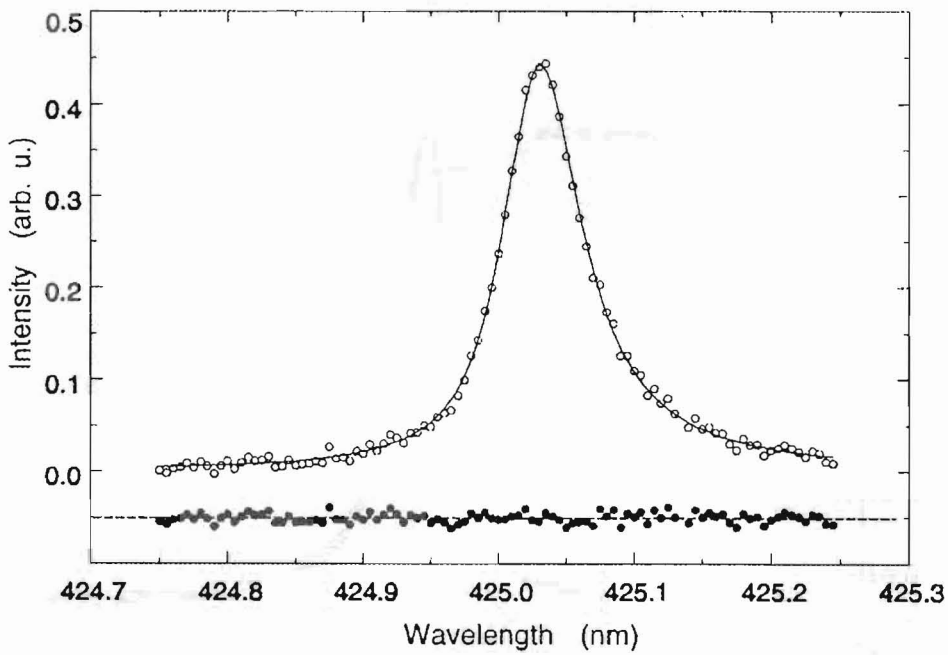

Fig. 2. Comparison of the randomly disturbed synthetic convolution (∘ ∘ ∘) with the model convolution (——) generated with an optimized set of adjustable parameters: $w_e = 0.0265$ nm, $d_e = 0.0217$ nm, $\gamma = 0.117$ and $C_n = 0.5025$ arb.u. · nm, at the end of the fitting. Diferences between those two convolutions (• • •) exibit random scatering.

The estimated covariance matrix of the performed fitting procedure has the form given in Table 1. According to Press et al. (1995), the 68.3% confidence intervals for the values of the fitted parameters are: $\delta w_e = 0.0012$ nm, $\delta d_e = 0.0013$ nm, $\delta\gamma = 0.021$ and $\delta C_n = 0.011$ arb.u.·nm

Table 1. Elements of the covariance matrix necessary for the estimation of the model parameters standard deviations

[C]	w_e (10^{-1} nm)	d_e (10^{-1} nm)	γ	C_n (arb.u.·nm)
w_e (10^{-1} nm)	$3.08\cdot10^{-5}$	$1.38\cdot10^{-5}$	$-3.57\cdot10^{-5}$	$1.4\cdot10^{-5}$
d_e (10^{-1} nm)	$1.38\cdot10^{-5}$	$3.54\cdot10^{-5}$	$-4.55\cdot10^{-5}$	$5\cdot10^{-6}$
γ	$-3.57\cdot10^{-5}$	$-4.55\cdot10^{-5}$	$8.96\cdot10^{-5}$	$2.2\cdot10^{-6}$
C_n (arb.u.·nm)	$1.4\cdot10^{-5}$	$5\cdot10^{-6}$	$2.2\cdot10^{-6}$	$2.48\cdot10^{-5}$

7. RESULTS AND DISCUSSION

For the demonstrating purpose, some results (Nikolić, 1998) of exposed modeling method for the neutral argon spectral will be presented. In the case of the isolated ArI lines, the 425.9 nm spectral line is selected and given in Fig. 3.

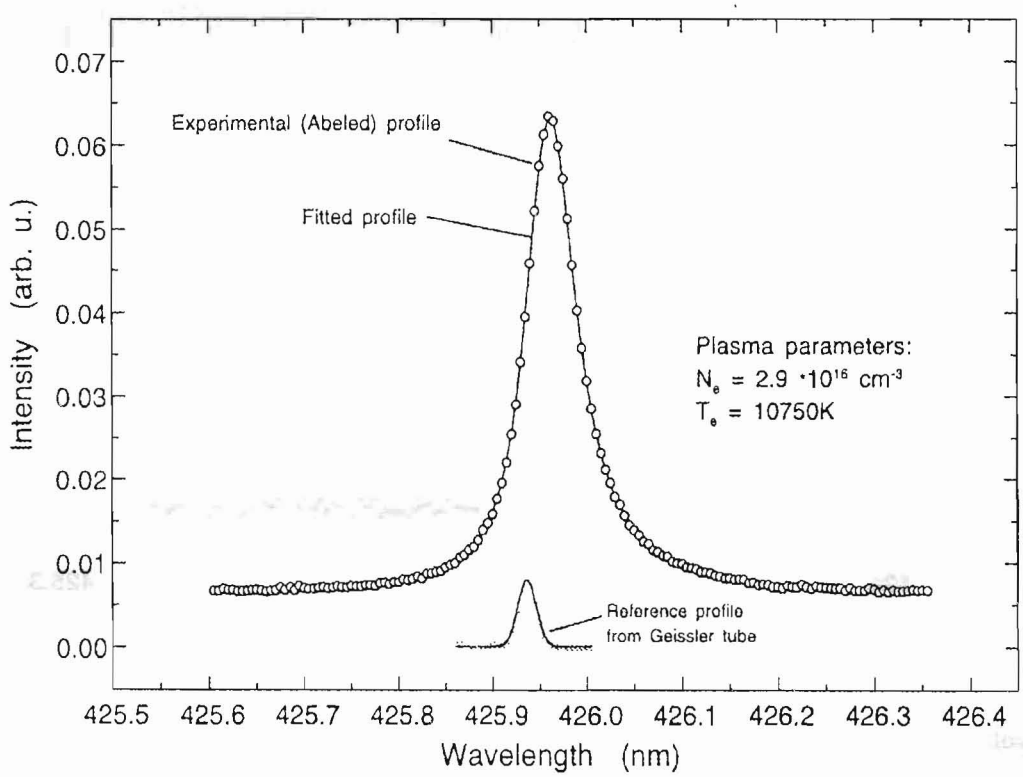

Fig. 3. Demonstration of fitting procedure in the case of Ar I 425.9 nm spectral line (Nikolić, 1998)

As representatives of two significantly overlapped neutral argon lines, Ar I 419.07 nm and Ar I 419.10 nm were taken (Nikolić et al., 1999). The final result of fitting procedure for these lines is illustrated in Fig.4.

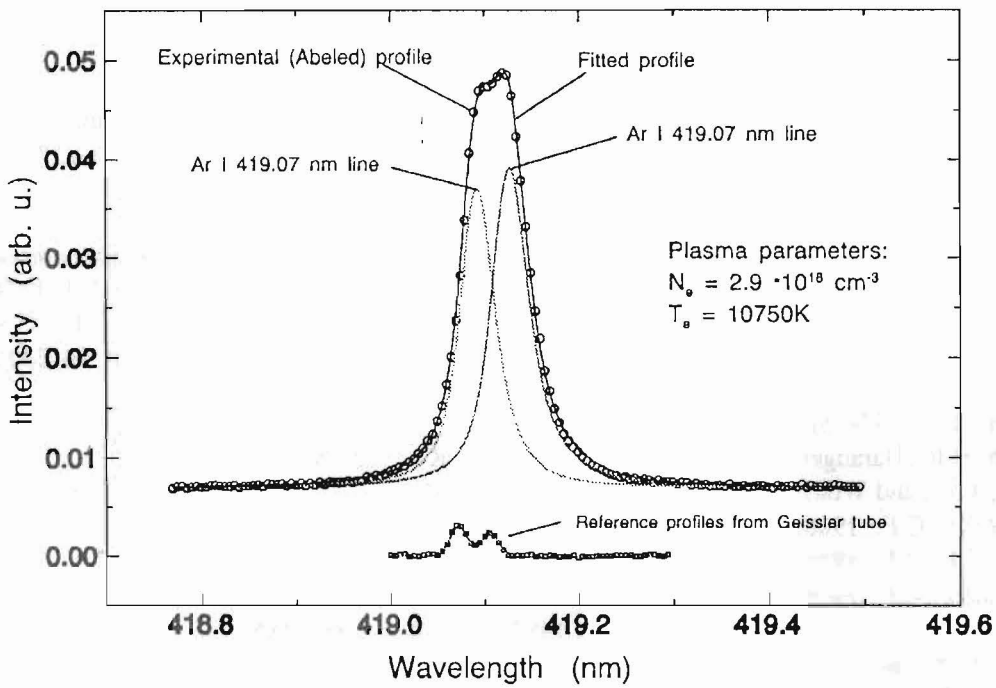

Fig. 4. Demonstration of fitting procedure in the case of two overlapped Ar I 419.07 nm and Ar I 419.10 nm spectral line (Nikolić, 1998)

As it can be seen from presented examples, described method results in fitted profiles which are in very good agreement with the experimental one. The only drawback of this method is long computing time - few hours for two overlapping lines - on pentium based PC with 32 MB RAM.

8. CONCLUSION

The herein presented method for modeling the spectral line shape of neutral atoms emitted from plasmas can be successfully applied under specified conditions. Existing theoretical predictions for Stark parameters of investigated spectral lines can be verified directly from high-precision measurements, providing proper separation of all significant broadening effects.

References

Badie, J.M., and Bacri, J.: 1991, *J. Phys. D* **24**, 809

Bakshi, V., and Kearney, R.J.: 1989, *J. Quant. Spectrosc. Radiat. Transfer* **42**, 405

Baranger, M., and Mozer, B.: 1959, *Phys. Rev.* **115**, 521

Brandt, T., Helbig, V., and Nick, K.P.: 1981, in: *Spectral Line Shapes* (B. Wende, Editor), 265, Walter de Gruyter, Berlin

Davies, J.T., and Vaughan, J.M.: 1963, *Astrophys. J.* **137**, 1302

Draper, N.R., and Smith, H.: 1966, *Applied Regression Analysis*, John Wiley&Sons, Inc., N.Y.

Fuhr, J.R., and Lesage, A.: 1993, *Bibliography on Atomic Line Shapes and Shifts (July 1978 through March 1992)*, National Standards Reference Data Series, National Bureau of Standards, U.S. Government Printing Office, Washington, DC

Fuhr, J.R., Wiese, W.L., and Roszman, L.J.: 1972, *Bibliography on Atomic Line Shapes and Shifts*, Natl. Bur. Stds. Spec. Publ. 366; ibid. Suppl. 1 (1974); Suppl. 2 (1975); Suppl. 3 (1978)

Goly, A., and Grabowski, B.: 1976, *Zesz. Nauk. Wyzsz. Szk. Pedagog. Opolu, Fiz. No.* **17**, 93

Goly, A., and Weniger, S.: 1986, *J. Quant. Spectrosc. Radiat. Transfer* **36**, 147; ibid. **38**, 225 (1987)

Griem, H.R.: 1962, *Phys. Rev.* **128**, 515

Griem, H.R.: 1974, *Spectral Line Broadening by Plasmas*, Academic Press

Griem, H.R., Baranger, M., Kolb, A.C., and Oertel, G.K.: 1962, *Phys. Rev.* **125**, 177

Hahn, T.D., and Woltz, L.A.: 1990, *Phys. Rev. A* **42**, 1450

Hooper Jr., C.F.: 1966, *Phys. Rev.* **149**, 77

Hooper Jr., C.F.: 1968 *a*, *Phys. Rev.***165**, 215

Hooper Jr., C.F.: 1968 *b*, *Phys. Rev.* **169**, 193

Jones, D.W., Pichler, G., and Wiese, W.L.: 1987, *Phys. Rev. A* **35**, 2585

Jones, D.W., and Wiese, W.L.: 1984, *Phys. Rev. A* **30**, 2602

Jones, D.W., Wiese, W.L., and Woltz, L.A.: 1986, *Phys. Rev. A* **34**, 450

Kelleher, D.E.: 1981, *J. Quant. Spectrosc. Radiat. Transfer* **25**, 191

Knauer, J.P. and Kock, M.: 1996, *J. Quant. Spectrosc. Radiat. Transfer* **56**, 563

Konjević, N., and Roberts, J.R.: 1976, *J. Phys. Chem. Ref. Data* **5**, 209

Konjević, N., Dimitrijević, M.S., and Wiese, W.L.: 1984, *J. Phys. Chem. Ref. Data* **13**, 619; ibid. **19**, 1307 (1990)

Marquardt, D.W.: 1963, *J. Soc. Indust. Appl. Math.*, **2**, 431

Mijatović, Z., Kobilarov, R., Vujičić, B.T., Nikolić, D., and Konjević, N.: 1993, *J. Quant. Spectrosc. Radiat. Transfer* **50**, 329

Mozer, B., and Baranger, M.: 1960, *Phys. Rev.* **118**, 626

Nikolić, D.: 1998, '*Influence of plasma temperature on shape and shift of argon spectral lines*', MSc Thesis, University of Belgrade, Belgrade (in Serbian)

Nikolić, D., Djurović, S., Mijatović, Z., Kobilarov, R., and Konjević, N.: 1999, *14th International Conference on Spectral Line Shapes* (Ed. R. Herman), AIP, New York, **10**, 191

Nikolić, D., Mijatović, Z., Djurović, S., Kobilarov, R., and Konjević, N.: 1998, *Deconvolution of Plasma Broadened Non-Hydrogenic Neutral Atom Lines*, accepted for publication in *J. Quant. Spectrosc. Radiat. Transfer*

Nubbemeyer, H.: 1980, *Phys. Rev. A* **22**, 1034

Press, W.H., Teukolsky, S.A., Vetterling, W.T., and Flannery, B.P.: 1995, *Numerical Recipes in C, Fortran and Pascal, 2nd ed.*, Cambridge University Press

Roder, O., and Stampa, A.: 1964, *Z. Physik* **178**, 348

Schinkoth, D., Kock, M., and Schulz-Gulde, E.: 1998, 'Experimental Stark Broadening Parameters for Near-Infrared Ar I and Kr I Lines', submitted to *J. Quant. Spectrosc. Radiat. Transfer*

Wolfram, S.: 1996, *The Mathematica Book, 3rd ed.*, Wolfram Media / Cambridge University Press)

Woltz, L.A.: 1986, *J. Quant. Spectrosc. Radiat. Transfer* **36**, 547